Calculation of quasi dispersion curves and quality factors of coupled resonator optical waveguides in photonic-crystal slabs

Chih-Hsien Huang,[1,2,3] Wei-Shuo Li,[1] Jing-Nuo Wu,[4] Wen-Feng Hsieh,[1,5] and Yia-Chung Chang[1,2,6]

[1]*Department of Photonics, National Chiao Tung University, Hsinchu 300, Taiwan*
[2]*Research Centre for Applied Sciences, Academia Sinica, Taipei 115, Taiwan*
[3]*Light Source Division, National Synchrotron Radiation Research Center, Hsinchu 300, Taiwan*
[4]*Department of Physics, Chinese Culture University, Taipei 111, Taiwan*
[5]*e-mail:wfhsieh@mail.nctu.edu.tw*
[6]*e-mail:yiachang@gate.sinica.edu.tw*

Received March 7, 2012; revised June 7, 2012; accepted July 31, 2012;
posted July 31, 2012 (Doc. ID 164049); published August 28, 2012

We propose a stabilization method to numerically calculate the dispersion relations and quality factors of optically confined finite structures. For the coupled resonator optical waveguide (CROW) made in a photonic-crystal slab (PCS) used as an example, the dispersion curve is normally not well defined due to the appearance of discontinuities, which do not occur in a two-dimensional CROW with infinite slab height. Therefore, there is less effort devoted to the calculation of quasi dispersion curves of the CROW in a slab. The dispersion relation of the PCS CROW can only be obtained by theoretical fitting to the experimental data under the tight-binding approximation. Here, we demonstrate the use of a stabilization method to calculate the quasi dispersion relation of a PCS CROW accurately. From the stabilization graph, we can calculate the quality factor for an eigenfrequency and properly choose the size of the simulation cell to avoid coupling the CROW modes with the unconfined modes and to accurately calculate the dispersion curve of the PCS CROW using the plane-wave expansion method. The proposed method and results not only provide important information for designing practical photonic devices such as slow-light optical waveguides and nonlinear photonic devices for the PCS CROWs but also can be applied to compute the quality factors and resonance frequencies of microcavities or nanocavities.

OCIS codes: 200.4490, 230.1150, 230.5298, 230.7400.

1. INTRODUCTION

Photonic crystals (PCs) [1] are periodic structures that give rise to bandgaps, which can be used to modify light propagation [2]. The coupled resonator optical waveguide (CROW) [3–6] or coupled cavity waveguide [7–9], which is a promising slow light device, can be fabricated by creating some point defects or cavities periodically along the wave propagation direction in a PC. Because the speed of light in a CROW is largely reduced [10,11], the nonlinear effect is largely enhanced [10,12,13] and the quantum dynamics of atoms embedded in CROWs are quite different from the Markovian decay [14]. Especially after the experimental demonstration of an ultraslow pulse propagation and a long group delay in a CROW by Notomi *et al.* [15], the practical optical devices [16,17] fabricated by CROWs become realizable.

The dispersion relation of a CROW is usually derived by the tight-binding method (TBM) [3] or transform matrix method (TMM) theoretically [18], which provides an analytical equation to further analyze the properties of a CROW, such as the pulse propagation within it or the interaction between light and material when quantum dots or nonlinear materials are added inside the defects [4,12,13]. To calculate the dispersion of a CROW by the TBM or TMM, the properties of a single cavity, such as electric field distribution and eigenfrequency, must be well defined. It is quite easy in a two-dimensional (2D) case, in which the height is supposedly infinite. However, in a practice device, the height of the PC slab (PCS) is finite and comparable to the lattice constant [19], and the simulation of a point defect becomes time consuming. In addition, the eigenfrequency of a point defect cannot be exactly defined [20,21] due to the finite quality factor unless the resonant frequency and the spectral width of the defect are both known in advance. Therefore, numerical studies of the dispersion curves of CROWs are mostly restricted to the 2D cases, and to our knowledge, a numerical method to calculate the dispersion relation of the CROW in a PCS is still lacking and the dispersion curves of CROWs are typically obtained by theoretical fitting to the experimental data [15]. The main difficulty is that the simulation results vary with the simulation condition, and the dispersion relation of the CROWs cannot be exactly obtained, so there only exists a quasi dispersion curve in the CROW. However, the dispersion relation determining the performance of the device should be known before fabricating a practice device. Therefore, it is desirable to have a method that can rigorously calculate the quasi dispersion curves and the properties of a PCS CROW.

In this paper, we first use the plane-wave expansion method (PWEM) [22] to calculate the dispersion curves of guided modes for a PCS CROW. Because the simulation super cell must be chosen to prevent field overlapping under the periodic boundary condition, it has an air cladding encompassing the PCS structure in the z direction (slab height) and a large

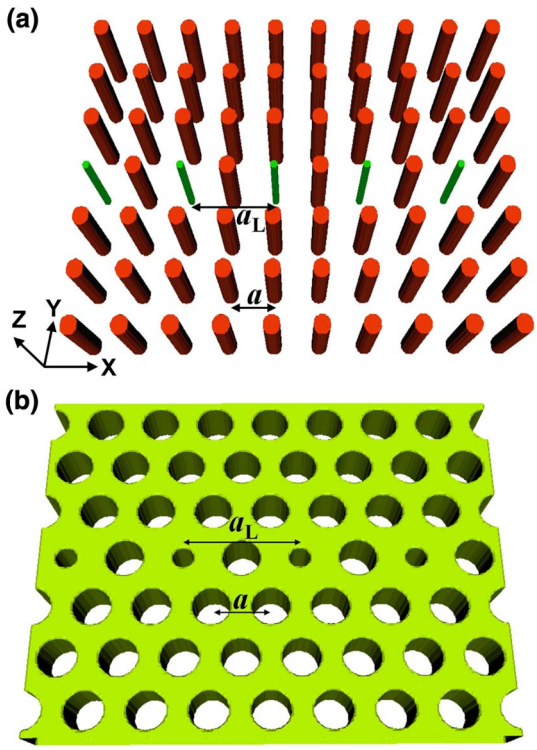

Fig. 1. (Color online) Structures of the coupled resonator optical waveguide (CROW) made of photonic-crystal slabs with (a) dielectric rods and (b) air holes. a and a_L are the lattice constants of photonic crystals and CROWs, respectively.

enough dimension in y direction, which is transverse to the CROW propagation (x) direction, as in Fig. 1. With this super cell, there are three kinds of optical modes, i.e., cavity-guided mode (CGM), slab-confined modes (SCMs), and unconfined modes (UCMs), existing in the super cell of a CROW made of a PCS for numerical simulation. For the CGM, its electric field is not only confined by the slab but also localized around the cavity (point defect) region without extending far into either the air cladding or the perfect photonic-crystal region. Here, we also named it the CROW guided mode, for this mode reveals the physical properties of the CROW structure. The SCM is a slab waveguide mode, which is confined in the z direction (slab height) via the total internal reflection (TIR), but it extends over the entire slab in the x and y directions except the cavity region. The optical field of the UCM extends over the entire super cell and is actually a radiation mode.

From the simulation results done by the PWEM, we found a distinct jump in the dispersion curve for some particular sizes of simulation cells, and the location of the frequency jump varies with the choice of simulation cell size. It indicates that the jump in the dispersion curve is a result of coupling of the CROW guided modes or CGMs to the UCMs in the air. The resonant coupling between the CGM and UCM can happen when the incident optical wave approaches the degenerate eigenfrequency of these two modes; it causes the energy transfer from the CGM to the UCM and anticrossing of the dispersion curves. The resonant coupling leads to energy leakage of the CGM to the UCM and eventually to the air as it propagates along the PCS CROW.

The leakage of electromagnetic (EM) waves into the air results in a quasi dispersion curve with a finite spectral width in an eigenfrequency. In order to evaluate the eigenfrequency and quality factor of the CROW guided mode, we adopt a stabilization method [23,24] that has commonly been used in the field of condensed matter physics. This stabilization method can be used to calculate the eigenfrequency and quality factor of an optically confined finite structure. From knowing the stabilization characteristics of PCS CROW, we can properly choose the size of the simulation cell to calculate the dispersion curve of the PCS CROW using the PWEM by avoiding the dispersion discontinuities caused by coupling of the CROW modes with the UCMs. Finally, the results are also compared with the 2D cases to discuss their physical insight and to give a primary design concept of CROWs by only doing 2D simulation.

2. QUASI DISPERSION CURVES

We consider CROWs made of either finite dielectric rods or air holes in a dielectric slab of thickness t_z, as shown in Fig. 1, in which the lattice constant of the perfect PCs is a and the distance between two adjacent defects of the CROWs is a_L. There exists a bandgap in TM-like mode for dielectric-rod structures and TE-like mode for the air-hole structures [20,25], so we shall only consider the polarization that gives rise to a bandgap.

To realize the CROW guided modes within the PCS whose dispersion curves lay below the light line (LL) [19], we first consider a CROW having a period $a_L = 2a$, which is made from a 2D PC (with rod radius $r = 0.2a$ and rod dielectric constant $\varepsilon = 12$ in a square lattice) by shrinking the rod radius to $r_d = 0.09a$ for every other rod in the middle row [see Fig. 1(a)]. Its dispersion curve in the extended Brillouin zone is shown in Fig. 2(a). For the CROW with $a_L = 2a$, there should be two dispersion curves in which the EM wave may localize in the defects. The breaking of translation symmetry with lattice constant a of the PC in the propagating (x) direction leads to the result that the two dispersion curves do not cross at $k_x = \pi/a_L$. In this CROW structure, because the partition rods between the defect rods in the PCW are identical to those made of the PC, one of the dispersion curves embeds in the dielectric band (below the bandgap). Thus we only observe one dispersion curve of the CROW guided mode in Fig. 2(a) located within the bandgap, which falls between $k_x = 0.65$ and 1 ($2\pi/a_L$). For the CROW with $a_L = 2a$, the first Brillouin zone (FBZ) boundary is located at π/a_L, and both the dispersion curve and LL can be folded into the FBZ. After the zone folding, the CROW guided modes exist for wave vectors in the range $k_x = 0$–0.35 ($2\pi/a_L$). The simulation approach for the CROWs with$a_L \geq 3a$ is similar to that with $a_L = 2a$, so in the following we only consider the CROW having $a_L = 2a$.

The dispersion curves of a PCS CROW with slab thickness $t_z = 2a$ are shown in Fig. 2(b). The super cell has the dimensions $2a \times 9a \times 4a$. It can be seen from the left inset of Fig. 2(b) that the electric field for the guided mode (solid curve) is localized within the defect rod and confined inside the slab. However, we also found the other modes within the photonic bandgap (dotted curves) in which the electric fields are not localized around the defect rod and extend over the entire super cell, as illustrated in the right inset in Fig. 2(b). The frequencies of these modes would be highly sensitive to the size of the chosen simulation unit cell or the boundary condition, and thus those are indentified as the UCMs. These UCMs will

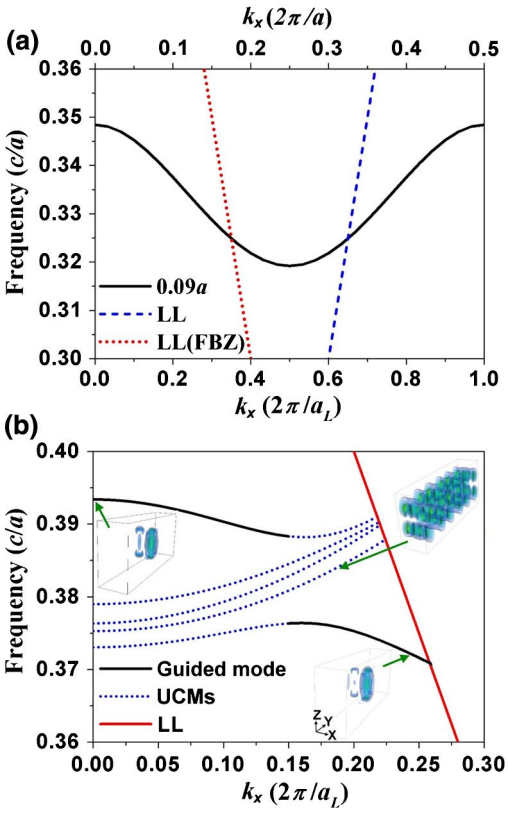

Fig. 2. (Color online) Dispersion curves of a CROW made of (a) a 2D dielectric-rod photonic crystal and (b) a photonic-crystal slab (PCS) calculated using a super cell of size $2a \times 9a \times 4a$. The insets in (b) illustrate the intensity distribution of the electric field.

interfere with the CROW guided mode or CGM, leading to a discontinuity (jump) in the dispersion curve of the guided mode for a PCS CROW (solid curve). The breaking translation symmetry with lattice constant a in the propagating direction leads to the dispersion curve of the guided mode folding into the FBZ that interacts with those UCMs. In other words, the jump of the dispersion curve is caused by the coupling of cavities with the air through the UCMs extending outside the slab into the air.

Near the frequency where the jump occurs, the EM field becomes delocalized and extends outside the cavities. In order to realize the interaction strength between the cavities and the air, we use a stabilization method [23,24] to calculate the dispersion curve and quality factor of the CROW guided mode. Because the eigenfrequency of the guided mode at a fixed wave vector should be independent of the size of the chosen simulation cell, but the UCMs with delocalized fields do depend upon the size of the chosen cell, we can obtain a stabilization graph, $f(z)$, which plots the eigenfrequency at $k_x = 0$ as a function of the height of the super cell with fixed $7a$ in the y direction as shown in Fig. 3(a). The flat curves correspond to the resonant frequency of the guided mode or other confined modes that barely change as the size of the simulation cell varies, unlike other curves corresponding to the UCMs that decrease with increasing simulation cell size. Here we distinguish the flat curves into two categories. One is the CGM or CROW guided mode, in which the EM wave localizes near the cavities and propagates inside the waveguide, e.g., the flat dispersion curve around $f = 0.389\,c/a$ in Fig. 3(a). The others are

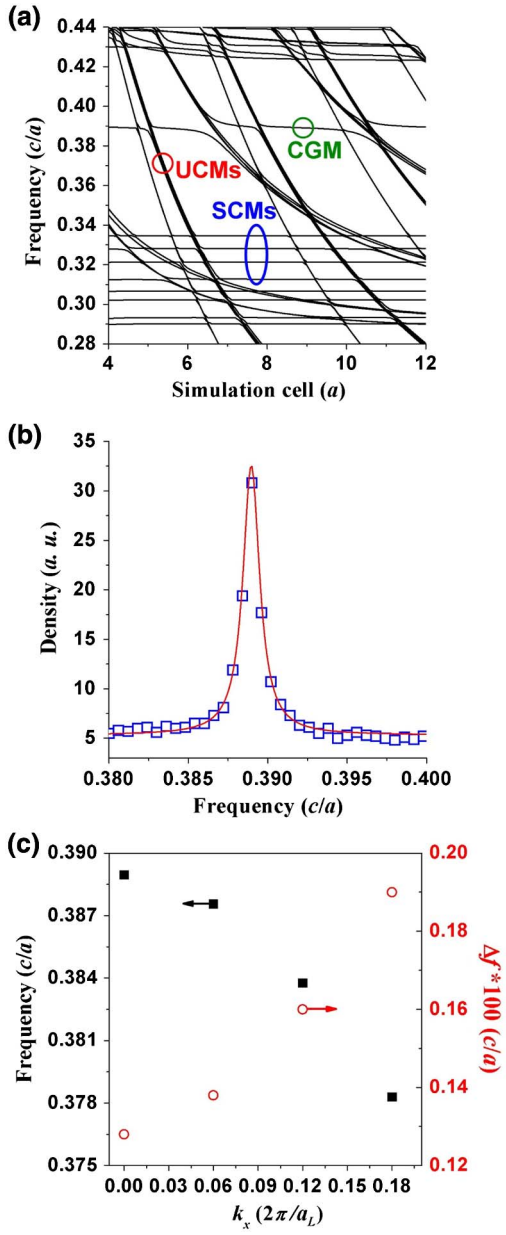

Fig. 3. (Color online) (a) Dispersion relation of the CROW at $k_x = 0$ using a simulation cell 4–12a in the z direction and (b) its resonant density. The flat curves in (a) are contributed by one cavity-guided mode (CGM) with f around $0.389\,c/a$ and several slab-confined modes (SCMs) in the allowed bands. The curves vary with simulation cell contributions from the unconfined modes (UCMs). (c) The eigenfrequency and spectral width Δf at each wave vector.

the SCMs, in which the EM wave mainly localizes within the slab, except the cavity region. The existence or number of these SCMs depends on the magnitude of the simulation cell in the y direction. The wave vectors of the reciprocal lattices in the y direction provide a tangential moment to allow the EM wave inside the slab. Note that the UCMs interact less with these SCMs but interact highly with the CGM, because the EM waves in the SCMs locate outside the cavity having translation symmetry of the lattice constant a in the propagation direction and the CGMs do not have this translation symmetry. Therefore, we can reduce the modification of the defects from the perfect rods or holes in the CROW to reduce the interaction by preserving the translation symmetry.

The stabilization method is based on calculating the size-averaged density of states (SDOS) by varying the length, z, of the simulation cell at a particular dimension shown in Fig. 3(b). The SDOS can be defined as [24]

$$\rho_z(f) = \frac{1}{\Delta z}\int_{z_0-\Delta z/2}^{z_0+\Delta z/2}\sum_i \delta(f - f_i(z))\mathrm{d}z = \frac{1}{\Delta z}\sum_i \left|\frac{df_i(z)}{dz}\right|^{-1}_{f_i(z_0)=f}. \quad (1)$$

Here $\sum_i \delta(f - f_i(z))$ is the density of state of the frequency f at simulation cell length z, i is the index of the calculated discrete eigenfrequencies shown in Fig. 3(a), z_0 is the simulation length, which contributes the density of state at frequency f, and Δz is the total simulation length, with which we calculate the density of state at each eigenfrequency. We have used

$$\int \mathrm{d}z\delta(f - f_i(z)) = \left|\frac{df_i(z)}{dz}\right|^{-1}_{f_i(z_0)=f}, \quad (2)$$

with $z - \Delta z/2 < z_0 < z + \Delta z/2$ in Eq. (1). The Δz must be long enough to have the sufficient number of eigenfrequencies satisfy the criterion $f_i(z_0) = f$ to avoid statistical error. From Eq. (1), it is clear that there are two methods to calculate the SDOS. In the first method, the SDOS at f is calculated by counting the number of eigenfrequencies at the entire simulation length $f_i(z)$, which has the same frequency as f. In the second method, the SDOS at f can also been obtained by taking the derivative of every frequency curve respectively to the simulation length z at f. The calculated SDOS consists of two types of contributions [23]:

$$\rho_z(f) = \rho_z^P(f) + \rho^Q(f), \quad (3)$$

where $\rho_z^P(f)$ denotes the background contribution (due to being coupled with modes of far away resonant frequencies), which varies smoothly with frequency and is relatively weak compared with $\rho^Q(f)$ near the resonant frequency. $\rho^Q(f)$ denotes the resonant contribution that can be well fitted by the Lorentzian form,

$$\rho^Q(f) \sim \frac{\Delta f/2}{(f - f_0)^2 + \Delta f^2/4}, \quad (4)$$

because this kind of SDOS is contributed by the photon spontaneous emission outside the cavity. Here, f_0 is the eigenfrequency and Δf is the spectral width for a given wave vector k_x.

Using this Lorentzian fitting to the SDOS in Fig. 3(b), we can obtain an accurate evaluation of the resonance frequency and its spectral width of the CROW guided mode to $0.389\,c/a$ and $0.00128\,c/a$ at $k_x = 0$, respectively, corresponding to a quality factor of 304. It indicates the PCS CROW is still a high quality waveguide, although the dispersion curves of the CROW cannot be accurately obtained by the conventional method due to the finite quality factor of this waveguide. The spectral width increases as k_x increases, as shown in Fig. 3(c). This is because the dispersion curves approach the LL at large wave vectors and at which the EM wave is no longer well confined in the slab.

As we discussed above, the spectral width of the quasi dispersion curve of the CROW caused by the CGM interacting with UCMs can be diminished by reducing the radii difference or dielectric constant difference between the perfect rods and defect rods. However, the difference between the perfect rods and defect rods cannot be too small, because it leads the dispersion curves too close the dielectric band edge and the photonic band confinement becomes weak, which leads the EM wave leakage in the x and y directions. The other method to diminish the spectral width of the dispersion curve is to enlarge the size of the cavities, i.e., by using more than one defect rod (holes), to provide larger modal volume, because generally the quality factor of a cavity is proportional to the modal volume.

This stabilization method can be applied to numerically calculate the quality factors and resonant frequencies of any microcavities or nanocavities by varying magnitude of a one-dimensional simulation cell by adding the air outside the cavity. Furthermore, the stabilization graph in Fig. 3(a) can also provide a guideline for properly chosen dimensions to prevent coupling of the CROW cavity mode with the UCMs. For instance, one could choose $9a$ in the z direction and $7a$ in the y direction, because the eigenfrequency of the CROW cavity mode is well separated from those of the UCMs. Thus, one can calculate the quasi dispersion curve of the PCS CROW CGM by using PWEM with a properly chosen super cell.

3. SIMULATION RESULTS OF PCW CROWS

In this section, we use the PWEM to calculate the CGM of the CROW by choosing properly and having a large enough super cell to avoid interaction with the UCM and cross talk between two CROWs due to the periodic boundary condition. In Fig. 4, we show a comparison of the CGM dispersion curves of 2D CROWs with those of PCS CROWs made of the dielectric rods and air holes calculated with a properly chosen simulation cell (which avoids the coupling of the guided mode with the UCMs). We found from Fig. 4(a) the dispersion curves of the CROWs made from dielectric-rod PCSs shift to the higher frequency nearly rigidly as compared with the 2D counterparts (with the same radii as the defect rods). This is because the evanescent waves would extend outside the slab, making the effective indices for the slab modes lower than their 2D counterparts, while the group velocity of the PCS CROW guided mode or CGM is approximately the same as that of the 2D counterpart. However, to obtain accurate dispersion curves for PCS CROWs, the 3D simulation by the PWEM is still needed.

For the CROWs made of defect holes with enlarged radii in the air-hole PCS or 2D PC, their dispersion curves are no longer parallel to each other, as shown in Fig. 4(b). The magnitude of the group velocity of the 2D CROW guided mode is larger than that of the PCS counterpart, as illustrated in the inset of Fig. 4(b), due to less confinement of the electric field in the defects. Because the electric field is not so localized within the defect holes but spread out in the dielectric region between the defect holes, the coupling between the next-neighbor defects [26] should be taken into consideration in the tight-binding theory, and it makes the dispersion curves bend downward at large wave vectors.

In Fig. 4(c), we note that when the defect holes are shrunk or replaced by a dielectric rod, the CROW becomes a two-mode waveguide with two crossing dispersion curves.

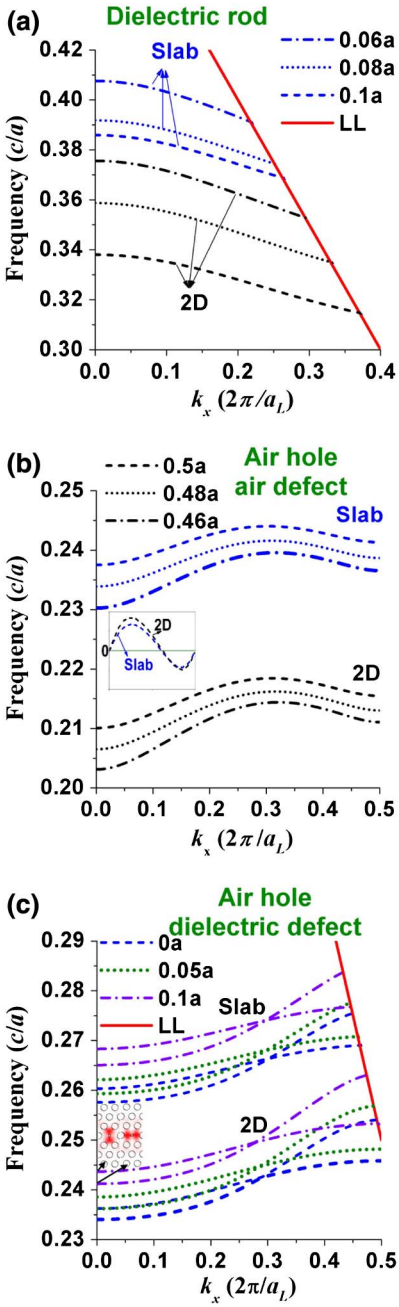

Fig. 4. (Color online) Comparison of dispersion curves of 2D CROWs and PCS CROWs made of either dielectric rods or air holes in a dielectric having a dielectric constant of 12. (a) Dielectric-rod CROWs with rod radius of $0.2a$ in the PC and a defect rod radius r_d ranging from 0.06 to $0.1a$. The slab height for the PCS is $2a$; (b) Air-hole CROWs with a hole radius of $0.3a$ in the triangular-lattice PC and a defect hole radius r_d ranging from 0.46 to $0.5a$. The slab height for the PCS is a; (c) Same PC as in (b) with a radius of defect holes r_d ranging from 0 to $0.1a$. The inset in (b) shows a comparison of group velocities of the two structures with $r_d = 0.5a$. The inset in (c) illustrates the intensity distribution of an EM wave for $r_d = 0.1a$.

The intensity distributions of two CROW guided modes are shown in the inset of Fig. 4(c). At low k_x, the low frequency mode is a longitudinal mode (having a longitudinal field distribution), whereas the other one is a transverse mode. The coupling strength of the longitudinal mode is larger than that of the transverse mode, and the stronger coupling strength gives rise to a higher group velocity.

4. CONCLUSION

We observe that the guided modes in CROWs made from a PCS have a finite lifetime, and thus can only be described by quasi dispersion curves with a finite width. By using the stabilization method, we can obtain the finite spectral width of the guided mode, which typically has a high quality factor so the EM wave can still propagate well in the CROW with low leakage into the air. The spectral width of the guided mode can be reduced by diminishing the breaking of the translation symmetrically along the propagation direction. By properly choosing the simulation cell to avoid strong interaction with the unconfined modes, the dispersion curve of the CROW guided mode or cavity-guided mode become less sensitive to the simulation cell dimensions and its approximate dispersion curve can be obtained. For the CROW made of dielectric rods, the dispersion curve of the CROW guided mode is nearly parallel to the 2D counterpart. However, for the CROW made of air holes, this is no longer the case, due to different localization of the EM waves in the defects. The dispersion relation cannot be well described by the traditional tight-binding method, in which the nearest-neighbor defect coupling is considered only, due to the reduced confinement of the electric field. When the defect holes are shrunk or replaced by a dielectric rod, the CROW becomes a double-mode waveguide with different group velocities for the two guided modes (one longitudinal and one transverse). The longitudinal mode is found to have a larger group velocity because of the stronger coupling between two adjacent defects.

ACKNOWLEDGMENTS

This work is supported in part by X-Photonics Interdisciplinary Center of National Chiao Tung University and the National Science Council of China under grants NSC99-2112-M006-017-MY3, NSC99-2221-E009-095-MY3, and NSC98-2112-M-001-022-MY3.

REFERENCES

1. E. Yablonovitch, "Inhibited spontaneous emission on solid-state physics and electronics," Phys. Rev. Lett. **58**, 2059–2062 (1987).
2. S. Y. Lin, E. Chow, J. Bur, S. G. Johnson, and J. D. Joannopoulos, "Low-loss, wide-angle Y splitter ~1.6 μm wavelengths built with a two-dimensional photonic crystal," Opt. Lett. **27**, 1400–1402 (2002).
3. A. Yariv, Y. Xu, R. K. Lee, and A. Scherer, "Coupled-resonator optical waveguide: a proposal and analysis," Opt. Lett. **24**, 711–713 (1999).
4. D. N. Christodoulides and N. K. Efremidis, "Discrete temporal solitons along a chain of nonlinear coupled microcavities embedded in photonic crystals," Opt. Lett. **27**, 568–570 (2002).
5. C. F. Ouyang, Z. Q. Xiong, F. Y. Zhao, B. Q. Dong, X. H. Hu, X. H. Liu, and J. Zi, "Slow light with low group-velocity dispersion at the edge of photonic graphene," Phys. Rev. A **84**, 015801 (2011).
6. K. H. Tian, W. Arora, S. Takahashi, J. Hong, and G. Barbastathis, "Dynamic group velocity control in a mechanically tunable photonic-crystal coupled-resonator optical waveguide," Phys. Rev. B **80**, 134305 (2009).
7. M. Bayindir and E. Ozbay, "Heavy photons at coupled-cavity waveguide band edges in a three-dimensional photonic crystal," Phys. Rev. B **62**, R2247–R2250 (2000).
8. M. Bayindir, B. Temelkuran, and E. Ozbay, "Tight-binding description of the coupled defect modes in three-dimensional photonic crystals," Phys. Rev. Lett. **84**, 2140–2143 (2000).
9. M. L. Cooper, G. Gupta, M. A. Schneider, W. M. J. Green, S. Assefa, F. N. A. Xia, D. K. Gifford, and S. Mookherjea, "Waveguide dispersion effects in silicon-on-insulator coupled-resonator optical waveguides," Opt. Lett. **35**, 3030–3032 (2010).

10. S. A. Schulz, L. O'Faolain, D. M. Beggs, T. P. White, A. Melloni, and T. F. Krauss, "Dispersion engineered slow light in photonic crystals: a comparison," J. Opt. **12**, 104004 (2010).
11. A. Talneau, "Slow light modes for optical delay lines: 2D photonic crystal-based design structures, performances and challenges," J. Opt. **12**, 104005 (2010).
12. C. H. Huang, Y. H. Lai, S. C. Cheng, and W. F. Hsieh, "Modulation instability in nonlinear coupled resonator optical waveguides and photonic crystal waveguides," Opt. Express **17**, 1299–1307 (2009).
13. C. H. Huang, J. N. Wu, S. C. Cheng, and W. F. Hsieh, "The evolution of solitons in coupled resonator optical waveguides and photonic-crystal waveguides," Comput. Phys. Commun. **182**, 232–236 (2011).
14. D. P. Fussell and M. M. Dignam, "Quantum-dot photon dynamics in a coupled-cavity waveguide: observing band-edge quantum optics," Phys. Rev. A **76**, 053801 (2007).
15. M. Notomi, E. Kuramochi, and T. Tanabe, "Large-scale arrays of ultrahigh-*Q* coupled nanocavities," Nat. Photon. **2**, 741–747 (2008).
16. C. Agger, T. S. Skovgard, N. Gregersen, and J. Mork, "Modeling of mode-locked coupled-resonator optical waveguide lasers," IEEE J. Quantum Electron. **46**, 1804–1812 (2010).
17. H. C. Liu and A. Yariv, "Synthesis of high-order bandpass filters based on coupled-resonator optical waveguides (CROWs)," Opt. Express **19**, 17653–17668 (2011).
18. J. K. S. Poon, J. Scheuer, S. Mookherjea, G. T. Paloczi, Y. Y. Huang, and A. Yariv, "Matrix analysis of microring coupled-resonator optical waveguides," Opt. Express **12**, 90–103 (2004).
19. S. G. Johnson, S. H. Fan, P. R. Villeneuve, J. D. Joannopoulos, and L. A. Kolodziejski, "Guided modes in photonic crystal slabs," Phys. Rev. B **60**, 5751–5758 (1999).
20. J. D. Joannopoulos, S. G. Johnson, J. N. Winn, and R. D. Meade, *Photonic Crystals: Modeling the Flow of Light* (Princeton University, 2008).
21. S. G. Johnson and J. D. Joannopoulos, *Photonic Crystals: the Road from Theory to Practice* (Kluwer Academic, 2002), pp. 99–112.
22. S. G. Johnson and J. D. Joannopoulos, "Block-iterative frequency-domain methods for Maxwell's equations in a plane-wave basis," Opt. Express **8**, 173–190 (2001).
23. V. A. Mandelshtam, T. R. Ravuri, and H. S. Taylor, "Calculation of the density of resonance states using the stabilization method," Phys. Rev. Lett. **70**, 1932–1935 (1993).
24. D. M. T. Kuo and Y. C. Chang, "Electron tunneling rate in quantum dots under a uniform electric field," Phys. Rev. B **61**, 11051–11056 (2000).
25. E. Chow, S. Y. Lin, S. G. Johnson, P. R. Villeneuve, J. D. Joannopoulos, J. R. Wendt, G. A. Vawter, W. Zubrzycki, H. Hou, and A. Alleman, "Three-dimensional control of light in a two-dimensional photonic crystal slab," Nature **407**, 983–986 (2000).
26. C. H. Huang, J. N. Wu, P. Y. Lee, W. F. Hsieh, and S. C. Cheng, "The properties and design concepts of photonic directional couplers made of photonic crystal slabs," J. Phys. D **43**, 465103 (2010).